Characterization of tin selenide nanoparticle films generating from plasma arc penetration of a temperature-varying field

Hakima A. Abdulla, Nadheer Jassim Mohammed, Aseel Mustafa Abdul Majeed
Department of Physics, College of Science, Mustansiriyah University, Baghdad, Iraq

Article Info

ABSTRACT

Using the pulsed laser deposition (PLD) method, tin selenide (SnSe) nanoparticles thin films are created on quartz substrates, which are held at different penetration field temperatures Tp-f (Tp-f is the penetration field temperature to which the plasma arc is exposed) (300, 373, 473, and 573) K. X-ray powder diffraction (XRD) reveals a phase transformation from a hexagonal to an orthorhombic structure. The energy gap, which ranges from 1.748-3.15 eV with direct electronic transmission, is calculated using transmittance spectra. Particle size increases by Tp-f increases. Photoluminescence (PL) intensity and film thickness are inversely proportional to each other. Changing the ratio of the compositions provides an essential strategy for altering a material's melting point as well as its energy gap.

Corresponding Author:

Hakima A. Abdulla
Department of Physics, College of Sciences, Mustansiriyah University
Baghdad, Iraq
Email: hakima2983@uomustansiriyah.edu.iq

1. INTRODUCTION

Tin selenide (SnSe) is one of the semiconductor materials that attract scientific interest due to its unique properties (optical and electrical). Compound SnSe belongs to the (IV-VI) group with a narrow energy band gap. It is recognized with a chemical stability, and high absorption coefficient. Because of its non-toxicity and its availability in nature, it is safe and easy for human use. It has a melting point of 860 ℃, and an orthorhombic structure. Pmna is the space group of SnSe. The parameters of lattice for tin selenide are: a =11.496 Å, b=4.15 Å, and c=4.44 Å, various stoichiometry such as SnSe, $SnSe_2$, and Sn_2Se_3, lowering the photo corrosion process, unexciting semiconductor [1]–[9].

SnSe has many applications in a solar cell, holographic recording systems, memory switching devices, analytical voltammetry, optoelectronics, and electronics materials [1], [3], [5], [6], [10]–[24]. The present study reports the preparation of Tin Selenide nanoparticles thin film under high vacuum is about 10^{-5} mbar by the pulsed laser deposition (PLD) method, and examining how the temperature of the penetration field (T_{p-f}) affects their optical and structural characteristics.

2. METHOD

Figure 1 illustrates the PLD system setup and schem of penetration field temperature (T_{p-f}). The polycrystalline SnSe represents a material target. It is synthesized by taking an equal amount of 50% of both the elements Sn and Se and putting them in a quartz ampule in which a vacuum is created by a rotary 10^{-1} mbar. To prevent oxidation, the ampule is sealed and entered into a furnace at a temperature of 1,100 ℃ for 4 hours. The ampule is cooled to room temperature. Finally, to produce a pellet, the alloy is grounded and

compressed by a hydromechanical piston under 12 tons of pressure. The pellet has diameter of 12 mm and height of 4 mm. The pellet is characterized by X-ray powder diffraction (XRD) as a polycrystalline of the SnSe as shown in Figure 1(a).

Thin films of SnSe are deposited at a 45° angle on a quartz substrate at various penetration field temperatures (T_{p-f}) (300, 373, 473, and 573) K under a vacuum pressure of 3.5x10^{-5} mbar. A1064 nm is the wavelength of a Nd-Yag laser source. The laser repetition rate is 5 Hz, and energy of 600 mJ. The target and substrate both rotate at 6 rpm and have a separation distance of 3.5 cm. The plasma arc is exposed to a varying temperature filed as shown in Figure 1(b).
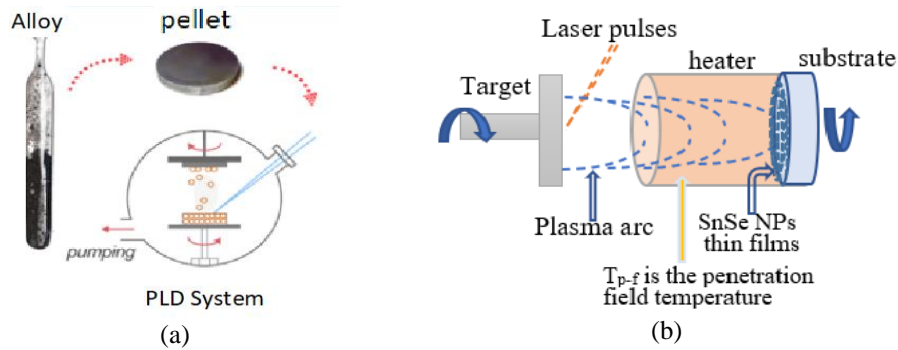

Figure 1. The PLD system setup and schem of penetration field temperature (T_{p-f}): (a) PLD setup [25] and (b) schem of pentration field temperature (T_{p-f})

3.   RESULTS AND DISCUSSION
3.1. Optical properties
3.1.1. Absorbance and transmittance spectra

Figure 2 shows the spectrum of absorbance and transmittance versus wavelength for SnSe deposited thin films at different T_{p-f} (300, 373, 473, and 573) K. The absorbance and transmittance spectra are very important to give us information about the energy gap value, which, according to it, we can choose the suitable application. Figures 2(a) and (b) shows the absorbance and transmittance spectra versus a wavelength ranging from 190–1100 nm as a function of penetration field temperature.
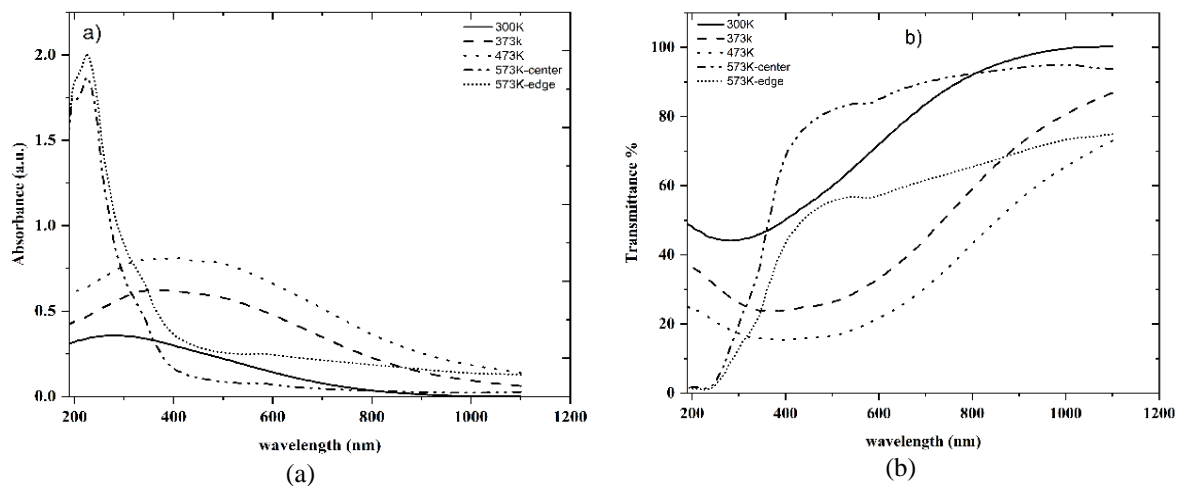

Figure 2. The spectrum of absorbance and transmittance versus wavelength for SnSe deposited thin films at different T_{p-f} (300, 373, 473, and 573) K: (a) absorbance and (b) transmittance

In Figure 2(a) the absorbance spectrum for specimens deposited at T_{p-f} (300, 373, and 473) K increases as the T_{p-f} rises and this is attributed to the increment of film thickness. The absorbance spectrum

peak shifts towards high wavelengths (low energies), except at 573 K, where it shifts towards low wavelengths (less than 400 nm). For the film which is prepared at 573 K, the absorbance is decreasing due to the lowering of the film thickness, but it increases in the region of wavelength (190-285) nm due to the high roughness. The full ultraviolet (UV) absorption, making the specimen created at 573 K suitable for UV detector applications.

In Figure 2(b) The transmittance spectrum is decreased with an increase in T_{p-f} to reach its lower value at a range of (190-600) nm, and the highest value at 1100 nm. The decrease in transmttance is due to an increase in film thickness, which produces a rise in both the density of localized states and the surface roughness [2]. At a T_{p-f} of 573 K, the transmittance spectrum reaches approximately 0% at wavelengths ranging (from 190–240) nm due to the full absorption, 72% or 99% at wavelengths between 240–1100 nm. This sharp increase in the transmittance spectrum indicates a direct transition to the conduction band. This action of transmittance and absorption is due to crystallinity enhancement [26].

The increasing or decreasing of the absorbance maxima spectra is supported by the images of the SnSe NPs thin film as in Figure 3. In the Figure 3, the shift in the wavelengths of the absorbance maxima towards high wavelengths is known as the "red shift ". Whereas the shift in the wavelengths of the absorbance maxima towards low wavelengths is known as "the blue shift".
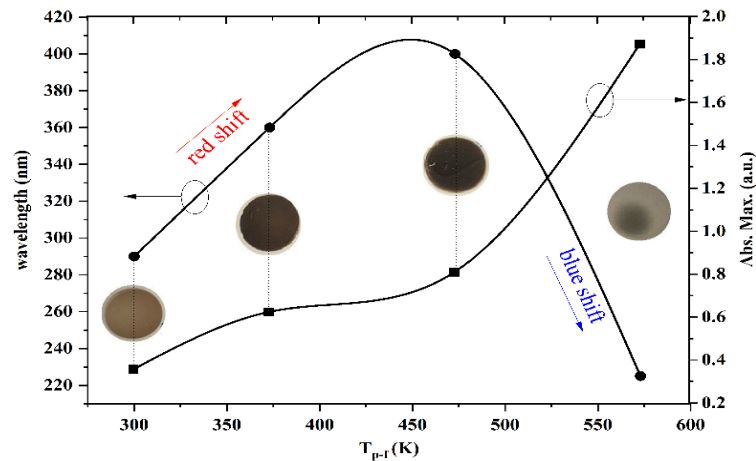

Figure 3. The red shift and blue shift for SnSe deposited thin films at different T_{p-f} (300, 373, 473, and 573) K

3.1.2. Absorption coefficient

Figure 4 shows the coefficient of absorption and $(\alpha h\nu)^2$ plot versus energy of the photon (eV) for SnSe deposited thin films at different T_{p-f} (300 K, 373 K, 473 K, 573 K). The absorption coefficient (α) is obtained from the below relationship [2]:

$$\alpha = -\frac{\ln(T)}{d} \tag{1}$$

where T and d denote transmittance of thin film and its thickness, respectively.

From the Figure 4(a), it is noticeable that the absorption coefficient (α) increases as the T_{p-f} increases, and its value for all the obtained thin films is larger than (10^4), which indicates the direct transition of electrons. Tauc's relation [27] was applied to determine the optical band gap energy for the SnSe thin films:

$$(\alpha h\nu) = \beta (h\nu - E.g) \tag{2}$$

where β is constant, n is dependent on the type of electron transition, so it is equal to (2) and (1/2) in the case of an indirect and a direct transition, respectively. E.g a material optical band gap.

By extrapolating to ($\alpha h\nu$)=0, Figure 4(b) the energy band gap ranged from (1.748-3.15) eV as in Table 1. The reduction of the energy band gap and then the rise with the increasing penetration field temperature is due to the improved crystallinity [28] and thickness increment of the thin films before the reduction of the film thickness happens [29].
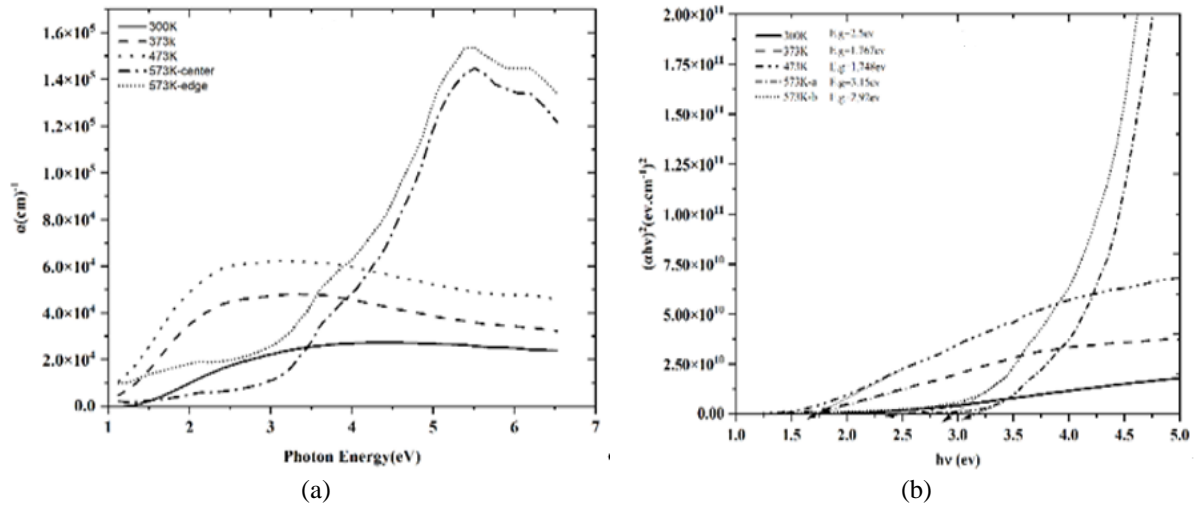
(a)   (b)

Figure 4. The coefficient of absorption and (αhv)2 plot versus energy of the photon (eV) for SnSe deposited thin films at different Tp-f (300 K, 373 K, 473 K, 573 K): (a) coefficient of absorption and (b) (αhv)2 plot versus energy of the photon (eV)

Table 1. The energy gap value of SnSe thin films

T_{p-f} (K)	300 K	373 K	473 K	573 K-center	573 K-edge
Energy gap value (eV)	2.5	1.767	1.748	3.152	2.92

3.1.3. Photoluminescence

There is a close relationship between the photoluminescence (PL) spectrum and the thickness of the layer of prepared thin films. PL is a function of the thickness of the layer, as they are inversely proportional. The thicker layer is the less intense peak of the photoluminescence, as shown in Figure 5, which correspond to the results obtained from [30]. The intensity of PL is 3 times lower than it was with the increase in the thin film thickness (decrease of defects) from one layer to 1.6 layers, as shown in Table 2.
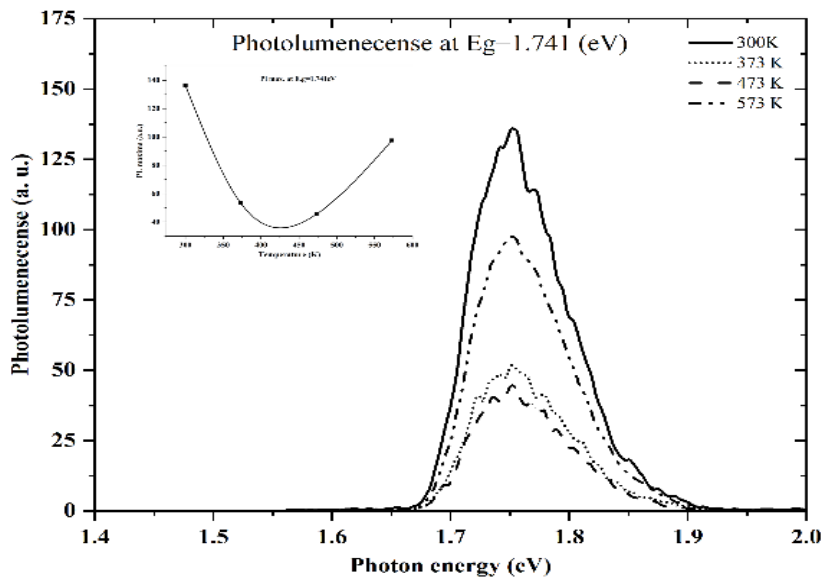

Figure 5. Photoluminescence (PL) of SnSe thin films vs. photon energy at different penetration field temperatures (300, 373, 473, and 573) K

Table 2. E.g, PL max, electron trap, film thickness of SnSe thin films

T_{p-f} (K)	E.g (eV)	PL max. (a.u)	Energy of electron trap (eV)	Film thickness (nm)
300	2.5	136.51	0.759	105
373	1.767	53.37	0.026	160
473	1.748	45.36	0.007	175
573	3.15	97.5	1.409	145

The surface of the monolayer thin film (the effect of the surface is meaning the process of oxidation, degradation, passivation, and other processes) has a significant influence on the impact on the optical properties of the monolayer. The optical properties of the obtained films are limited by the internal properties of the layers (such as composition, structure, layers' number, and defects), while the surface influence is negligible. The band gap is determined by the created thin films' thickness, which is determined by the layers' number. As a penetration field temperature rises, the thickness of the thin films grows, and the number of expanded energy levels will decrease the energy gap, reducing the photoluminescence spectrum.

The advantage of PL spectrum measurements can be regarded as a way to estimate the defects' presence in the film. The difference in energy between the optical energy gap and the PL spectra represents the amount of energy connecting the pair (electron-hole), which is known as an exciton. The Figure 6 illustrates that the electron emission of all deposited films corresponds to the wavelength value (712) nm.

The emissions are in the near infra-red zone (IRA). When the PL is generated, there is no change in the level at which electrons are transmitted. This indicates the purity of obtained films. These films are suitable for remote control applications due to their emission in IRA (the wavelength range for IRA is 700 to 1,400 nm).
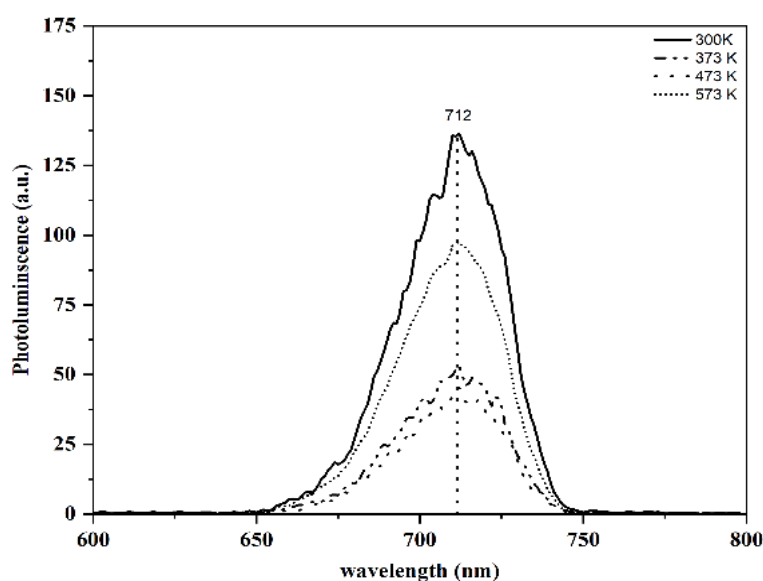

Figure 6. PL of SnSe thin films as a function of wavelength at different penetration field temperatures (300, 373, 473, and 573) K

3.2. Structural properties
3.2.1. X-ray diffraction

Figure 7 illustrates the x-ray diffraction patterns of PLD SnSe NP thin films coated on the substrate (quartz) at different penetration field temperatures. The X-ray diffraction pattern shows 15 to 75 2Θ values and it exhibits a phase transformation from a hexagonal to an orthorhombic structure. At low T_{p-f} (300) K, the obtained thin film contained $SnSe_2$ which has a hexagonal structure (JCPDS Card No. 00-023-0602). At a penetration field temperature rises to (373, 473, and 573) K the resulted films are contained SnSe with an orthorhombic structure (JCPDS Card No. 00-048-1244, which has lattice parameters: a = 11.49A °, b = 4.15A °, c = 4.44A°) as in Table 3. The presence of many peaks indicates that the resulted films have a polycrystalline system.

As the T_{p-f} increases, the crystalline size is increasing, while both the microstrain and dislocation density are decreased Table 3. In Figure 8 the change in films' compositions and the phase diagram of SnSe thin films deposited at various T_{p-f}. At a T_{p-f} of 300 K, the proportion of selenium was very high, so the obtained thin film had a hexagonal structure system. The orthorhombic system appears in all of the films manufactured at higher T_{p-f} (373, 473, and 573) K. This phase transformation from a hexagonal to an orthorhombic system that happened can be explained by the change in the film compositions, and the fact that the tin dioxide $SnSe_2$ is a poorly stable material. The tin content increased significantly as illustrated in Figure 8(a). When the T_{p-f} rises from 300 to 373 K, $SnSe_2$ transforms into a more stable structure (SnSe). A phase transformation is accomplished through the loss of selenium by evaporation [31] as in Table 4. The amount of energy required to break apart a crystal lattice is known as the melting point. The melting point of the crystal lattice is changing due to intermolecular motion, symmetry, rotation of molecules within the crystal, and the composition of the material [32].
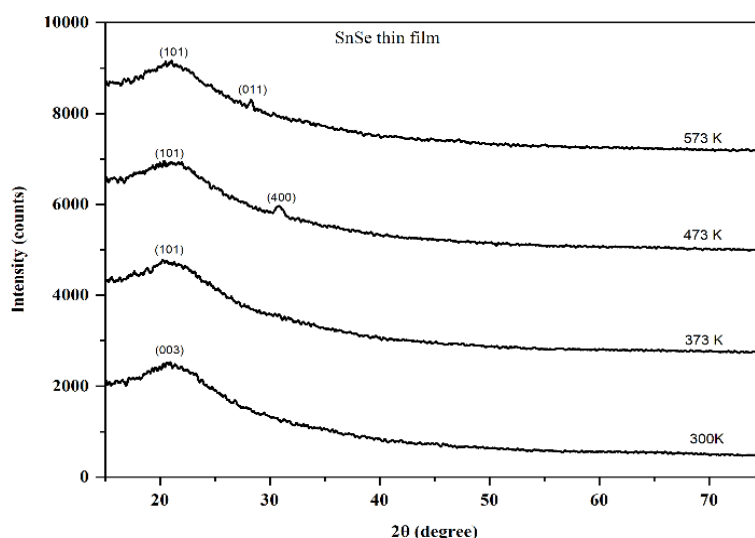

Figure 7. SnSe thin films' XRD curves at different T_{p-f} (300K, 373K, 473K, 573K)

Table 3. Structural properties for SnSe thin films at different penetration field temperature

T_{p-f} (K)	2theta (degree)	(hkl)	d-spacing (nm)	FWHM (degrees)	Crystalline size D (nm) (XRD)	Dislocation density δ (Lines/nm²)	Microstrain ε	structure	Chemical formula
300	21.63	(003)	4.10595	6	1.359	0.541	0.00500	Hexagonal	$SnSe_2$
373	21.7	(101)	4.09676	5.6	1.456	0.472	0.00468	Orthorhombic	SnSe
473	20.7	(101)	4.29621	4	2.042	0.240	0.00318	Orthorhombic	SnSe
473	30.81	(400)	2.90019	0.6	13.339	0.006	0.00072	Orthorhombic	SnSe
573	21.3	(101)	4.17777	3	2.720	0.1352	0.00246	Orthorhombic	SnSe
573	28.28	(011)	3.15354	0.07	115.004	0.0001	0.00008	Orthorhombic	SnSe

The melting point will be lower when the size is small and the crystal motion is fast. The melting point of $SnSe_2$ is smaller than that for SnSe, as seen in the Table 4. With a small crystal size, the number of molecules on the surface of the nanomaterial is large. The process of overcoming the internal forces of the crystal is facilitated and the melting point drops. The melting point of tin increases as the tin to selenium ratio increases. Figure 8(b) illustrates the phase diagram of SnSe NP thin film deposited at different T_{p-f}.

Table 4. Sn/Se ratio, the melting point of SnSe films at various penetration field temperatures

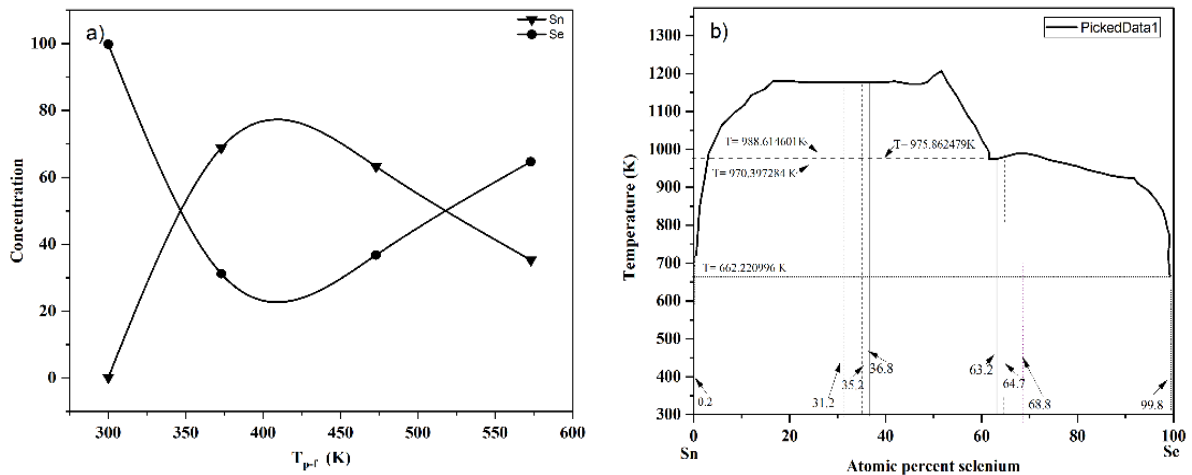| T_{p-f} (K)	Sn %	Se %	ratio of Sn/Se	Melting point (K)
300	0.2	99.8	0.002	662.22
373	68.8	31.2	2.205	988.61
473	63.2	36.8	1.717	970.39
573	35.3	64.7	0.546	975.86

Figure 8. The change in films' compositions and the phase diagram of SnSe thin films deposited at various penetration field temperatures: (a) the change in films' compositions and (b) the phase diagram of SnSe thin films (picked data1 adapted from the reference [33])

3.2.2. Field emission scanning electron microscopy (FESEM)

FESEM shows that the obtained films are all homogeneous Figure 9. Grain size increases at penetration field temperatures (300, 373, and 573) K as shown in Figures 9(a)-(d), but it decreases at T_{p-f} of 473 K. The energy gap of coated thin films drops as penetration field temperatures rise, except at 573 K where it increases due to the crystallinity change. The grain size is proportional inversely to the optical energy gap. As T_{p-f} increases, the crystalline size increases, and the number of energy levels that expand will reduce the energy gap [34].
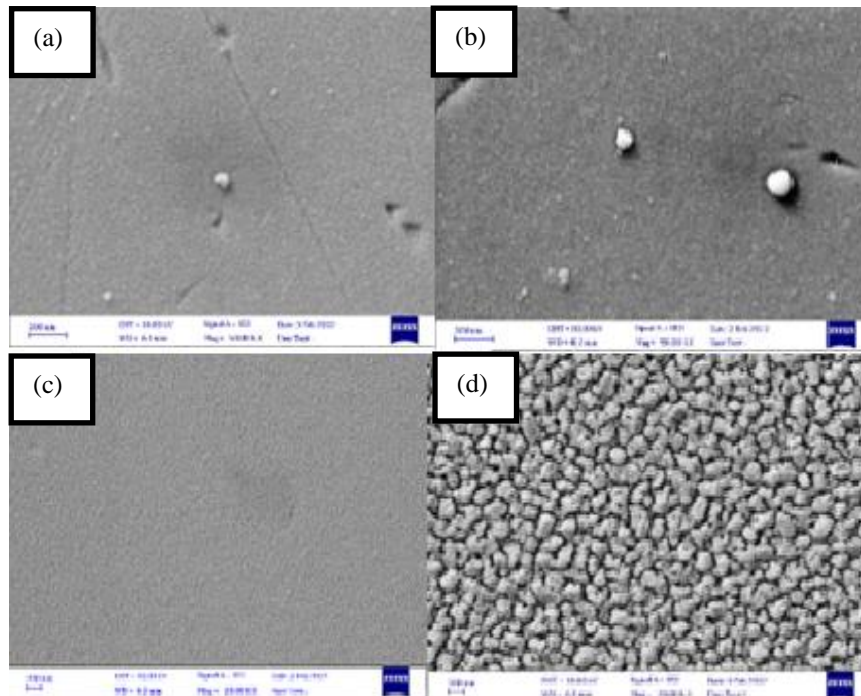
Figure 9. SnSe thin films' FESEM images at a different penetration field temperature: (a) 300 K, (b) 373 K, (c) 473 K, and (d) 573 K

4. CONCLUSION

Tin selenide NP thin films were coated on substrates made of quartz by using an effective method (PLD), which was held at various T_{p-f} (300 K, 373 K, 473 K, and 573 K). The transition from the red shift to the blue shift zone was shown in the absorbance spectrum data, which is suitable for manufacturing UV filter applications. The XRD pattern shows a phase transformation from a hexagonal structure at low penetration field temperature to an orthorhombic structure at (373, 473, and 573) K and all the resultant thin films were polycrystalline. Electron transmissions are direct with an energy gap of the deposited thin films (1.748–3.15) eV. The E.g decreases as the T_{p-f} rises, except at 573 K where it increases due to the crystallinity enhancement. Photoluminescence can be considered as a way to estimate the defects' presence in the thin film as it is a function of layer thickness. All films are pure and suitable for remote control applications due to their emission in IRA (712) nm, when PL is generated. All the obtained SnSe NP films were homogeneous, as illustrated by FESEM images.

REFERENCES

[1] S. Delice et al., "Temperature dependence of band gaps in sputtered SnSe thin films," *J. Phys. Chem. Solids*, vol. 131, no. January, pp. 22–26, 2019, doi: 10.1016/j.jpcs.2019.03.004.

[2] N. Kumar, U. Parihar, R. Kumar, K. J. Patel, C. J. Panchal, and N. Padha, "Effect of film thickness on optical properties of tin selenide thin films prepared by thermal evaporation for photovoltaic applications," *Am. J. Mater. Sci.*, vol. 2, no. 1, pp. 41–45, 2012, doi: 10.5923/j.materials.20120201.08.

[3] I. Lefebvre, M. Szymanski, J. Olivier-Fourcade, and J. Jumas, "Electronic structure of tin monochalcogenides from SnO to SnTe," *Phys. Rev. B - Condens. Matter Mater. Phys.*, vol. 58, no. 4, pp. 1896–1906, 1998, doi: 10.1103/PhysRevB.58.1896.

[4] C. W. Li et al., "Orbitally driven giant phonon anharmonicity in SnSe," *Nat. Phys.*, vol. 11, no. 12, pp. 1063–1069, 2015, doi: 10.1038/nphys3492.

[5] K. D. Patel, "Study and characterization of SnSe nanoparticles prepared by chemical bath method," no. February, 2017.

[6] F. Sava, M. Popescu, G. Socol, E. Axente, I. N. Mihailescu, and M. Nistor, "Amorphous SnSe 2 films," *J. Optoelectron. Adv. Mater.*, vol. 8, no. 4, pp. 1367–1371, 2006.

[7] V. R. Solanki, R. J. Parmar, R. J. Pathak, and M. D. Parmar, "Structural and optical properties of tin selenide thin films prepared by chemical bath deposition method," *AIP Conf. Proc.*, vol. 1837, no. February, pp. 1–4, 2017, doi: 10.1063/1.4982103.

[8] H. Yanuar, U. Lazuardi, and J. Copriady, "Preparation and characterization of thin film SnSe used by close spaced vapor transport technique," *Chalcogenide Lett.*, vol. 14, no. 5, pp. 181–185, 2017.

[9] L. D. Zhao et al., "Ultralow thermal conductivity and high thermoelectric figure of merit in SnSe crystals," *Nature*, vol. 508, no. 7496, pp. 373–377, 2014, doi: 10.1038/nature13184.

[10] V. Martelli, F. Abud, J. L. Jiménez, E. Baggio-Saitovich, L. D. Zhao, and K. Behnia, "Thermal diffusivity and its lower bound in orthorhombic SnSe," *Phys. Rev. B*, vol. 104, no. 3, pp. 1–7, 2021, doi: 10.1103/PhysRevB.104.035208.

[11] K. Nguyen-Cong, J. M. Gonzalez, B. A. Steele, and I. I. Oleynik, "Tin-selenium compounds at ambient and high pressures," *J. Phys. Chem. C*, vol. 122, no. 32, pp. 18274–18281, 2018, doi: 10.1021/acs.jpcc.8b04881.

[12] H. Okamoto, "Se-Sn (Selenium-Tin)," *J. Phase Equilibria*, vol. 19, no. 3, pp. 293–293, 1998, doi: 10.1361/105497198770342544.

[13] T. M. Razykov et al., "Characterisation of SnSe thin films fabricated by chemical molecular beam deposition for use in thin film solar cells," *Solar Energy*, vol. 159, pp. 834–840, 2018, doi: 10.1016/j.solener.2017.11.053.

[14] S. U. Rehman et al., "An insight into a novel cubic phase SnSe for prospective applications in optoelectronics and clean energy devices," *J. Alloys Compd.*, vol. 733, pp. 22–32, 2018, doi: 10.1016/j.jallcom.2017.10.192.

[15] R. C. Sharma and Y. A. Chang, "The Se-Sn System," *Bull. Alloy Phase Diagr.*, vol. 7, no. 1, pp. 68–72, 1986.

[16] K. S. Urmila, T. A. Namitha, J. Rajani, R. R. Philip, and B. Pradeep, "Optoelectronic properties and Seebeck coefficient in SnSe thin films," *J. Semicond.*, vol. 37, no. 9, 2016, doi: 10.1088/1674-4926/37/9/093002.

[17] Z. Zainal, S. Nagalingam, A. Kassim, M. Z. Hussein, and W. M. M. Yunus, "Effects of annealing on the properties of SnSe films," *Sol. Energy Mater. Sol. Cells*, vol. 81, no. 2, pp. 261–268, 2004, doi: 10.1016/j.solmat.2003.11.004.

[18] K. Zweibel, "Thin film PV manufacturing: Materials costs and their optimization," *Sol. Energy Mater. Sol. Cells*, vol. 63, no. 4, pp. 375–386, 2000, doi: 10.1016/S0927-0248(00)00057-X.

[19] G. S. Ahmed, B. K. H. Al-Maiyaly, B. H. Hussein, and H. K. Hassun, "Opto- electrical properties of p-SnSe:S/N-Si heterojunction for solar cell application," *AIP Conf. Proc.*, vol. 2307, no. December, 2020, doi: 10.1063/5.0033131.

[20] P. Beltrán-Bobadilla et al., "SnSe solar cells: current results and perspectives," *Gen. Chem.*, vol. 7, no. 1, pp. 200012–200012, 2021, doi: 10.21127/yaoyigc20200012.

[21] M. Bouška et al., "Pulsed laser deposited GeTe-rich GeTe-Sb2Te3 thin films," *Sci. Rep.*, vol. 6, pp. 1–10, 2016, doi: 10.1038/srep26552.

[22] U. Feleni et al., "Tin selenide quantum dots electrochemical biotransducer for the determination of indinavir - A protease inhibitor anti-retroviral drug," *J. Nano Res.*, vol. 45, pp. 12–24, 2017, doi: 10.4028/www.scientific.net/JNanoR.45.12.

[23] Y. Feutelais, M. Majid, B. Legendre, and S. G. Fries, "Phase diagram investigation and proposition of a thermodynamic evaluation of the tin-selenium system," *J. Phase Equilibria*, vol. 17, no. 1, pp. 40–49, 1996, doi: 10.1007/BF02648368.

[24] S. A. J. Jassim, A. A. R. A. Zumaila, and G. A. A. Al Waly, "Influence of substrate temperature on the structural, optical and electrical properties of CdS thin films deposited by thermal evaporation," *Results Phys.*, vol. 3, pp. 173–178, 2013, doi: 10.1016/j.rinp.2013.08.003.

[25] A. J. Hwaidi and N. J. Mohammed, "The improvement of structural and optical properties of WO 3 nanoparticles by regulation substrate-target distance in pulsed laser deposition technique," *Al-Mustansiriyah Journal of Science*, vol. 33, no. 2, pp. 103-107, 2022.

[26] A. Jebali, M. Ben Rabeh, N. Khemiri, and M. Kanzari, "The effect of substrate temperature on the optical properties of SnSb4S7 thin films," *Mater. Res. Bull.*, vol. 61, pp. 363–368, 2015, doi: 10.1016/j.materresbull.2014.10.047.

[27] S. Shimizu, K. Miwa, T. Kobayashi, Y. Tazawa, and S. Ono, "Oxidation-induced thermopower inversion in nanocrystalline SnSe thin film," *Sci. Rep.*, vol. 11, no. 1, pp. 1–8, 2021, doi: 10.1038/s41598-021-81195-7.

[28] N. Kumar *et al.,* "Influence of the substrate temperature on the structural, optical, and electrical properties of tin selenide thin films deposited by thermal evaporation method," *Cryst. Res. Technol.*, vol. 45, no. 1, pp. 53–58, 2010, doi: 10.1002/crat.200900424.

[29] A. Ohwofosirai, "A study of the optical conductivity, extinction coefficient and dielectric function of CdO by Sucessive ionic layer adsorption and reaction (SILAR) techniques," *Am. Chem. Sci. J.*, vol. 4, no. 6, pp. 736–744, 2014, doi: 10.9734/acsj/2014/6958.

[30] M. R. Molas *et al.,* "Photoluminescence as a probe of phosphorene properties," *npj 2D Mater. Appl.*, vol. 5, no. 1, pp. 1–24, 2021, doi: 10.1038/s41699-021-00263-8.

[31] S. H. Heo *et al.*, "Composition change-driven texturing and doping in solution-processed SnSe thermoelectric thin films," *Nat. Commun.*, vol. 10, no. 1, 2019, doi: 10.1038/s41467-019-08883-x.

[32] Y. Gogotsi, "Crystal growth and design 2001," *Growth (Lakeland)*, vol. 1, no. 3, pp. 6–8, 2001.

[33] M. Kumar, S. Rani, Y. Singh, K. S. Gour, and V. N. Singh, "Tin-selenide as a futuristic material: properties and applications," *RSC Adv.*, vol. 11, no. 12, pp. 6477–6503, 2021, doi: 10.1039/d0ra09807h.

[34] A. G. Kunjomana, J. Bibin, S. Varadharajaperumal, and M. Teena, "Control of physical vapor deposition and architecture of stoichiometric SnSe heterojunction structures for solar cells," *Vacuum*, vol. 191, no. November 2020, p. 110372, 2021, doi: 10.1016/j.vacuum.2021.110372.

BIOGRAPHIES OF AUTHORS

Hakima A. Abdulla ⓘ 🔵 SC ◖ is a M.Sc. student at college of science, Mustansiriyah University, Baghdad, Iraq. She received the B.Sc. degree in science of physics at 2009, from Mustansiriyah University, Baghdad, Iraq. She can be contacted at email: hakima2983@uomustansiriyah.edu.iq.

Prof. Dr. Nadheer Jassim Mohammed ⓘ 🔵 SC ◖ is Professor at college of Science, Mustansiriyah University, Iraq. He Holds a PhD degree in thin films by using electronic applications from Dagestan State University, Makhachkala, Russia, 2012. His research area is physical electronics. He is director of thin films and vacuum evaporation Research Lab. He has supervised and co-supervised 12 masters and 5 Ph.D. students. Dr Nadheer has filed a number of patents and industrial designs on his innovative ideas. His research interests include material science. He can be contacted at email: nadheerphys@uomustansiriyah.edu.iq.

Prof. Dr. Aseel Mustafa Abdul Majeed ⓘ 🔵 SC ◖ is Professor at college of Science, Mustansiriyah University, Iraq. She received the B.Sc. degree in science of physics at 1994, the M.Sc. degree at 2005, and the Ph.D. degree in science of physics at 2013 from Mustansiriyah University, Baghdad, Iraq. She has supervised and co-supervised 10 masters and 5 Ph.D. students. She has authored or coauthored 20 publications in Scopus, with 2 H-index and 20 citations. Her research interests include nanomaterials, solar cell, gas sensor, and cell line. She can be contacted at email: aseelalaziz@uomustansiriyah.edu.iq.